Quantum Oscillations and Polarization of Nuclear Spins in Photoexcited Triplet States

ARTICLE *in* THE JOURNAL OF PHYSICAL CHEMISTRY B · NOVEMBER 2010

Impact Factor: 3.3 · DOI: 10.1021/jp103508t · Source: PubMed

6 AUTHORS, INCLUDING:

Gerd Kothe
University of Freiburg
140 PUBLICATIONS **2,501** CITATIONS
SEE PROFILE

Michail Lukaschek
University of Freiburg
7 PUBLICATIONS **109** CITATIONS
SEE PROFILE

Quantum Oscillations and Polarization of Nuclear Spins in Photoexcited Triplet States[†]

Gerd Kothe,*[,‡] Tomoaki Yago,[‡,||] Jörg-Ulrich Weidner,[‡] Gerhard Link,[‡] Michail Lukaschek,[‡] and Tien-Sung Lin[§]

Department of Physical Chemistry, University of Freiburg, Albertstrasse 21, 79104 Freiburg, Germany, and Department of Chemistry, Washington University, One Brookings Drive, St. Louis, Missouri 63130

Received: April 19, 2010; Revised Manuscript Received: June 30, 2010

The unique physical properties of photoexcited triplet states have been explored in numerous spectroscopic studies employing electron paramagnetic resonance (EPR). So far, however, no quantum interference effects were found in these systems in the presence of a magnetic field. In this study, we report the successful EPR detection of nuclear quantum oscillations in an organic triplet state subject to an external magnetic field. The observed quantum coherences can be rationalized using an analytical theory. Analysis suggests that the nuclear spins are actively involved in the intersystem crossing process. The novel mechanism also acts as a source of oscillatory nuclear spin polarization that gives rise to large signal enhancement in nuclear magnetic resonance (NMR). This opens new perspectives for the analysis of chemically induced dynamic nuclear polarization in mechanistic studies of photoactive proteins.

Introduction

Upon photoexcitation of organic molecules, the lowest triplet state is populated by the intersystem crossing (ISC) from the first excited singlet. The dipolar interactions between the unpaired electron spins in the triplet state give rise to the zero-field splitting. Selective population of the zero-field spin sublevels according to the symmetry selection rules of spin−orbit coupling yields high electron spin polarization in an external field.[1] It has been shown that organic triplet states can be born at milli-Kelvin spin temperatures, even though the samples are held at room temperature. These unique properties of photoexcited triplet states have been exploited in the development of several new magnetic resonance techniques such as single-molecule optical-detected magnetic resonance,[2,3] dynamic nuclear polarization,[4−6] and zero-field EPR combined with fast-field sweeping.[7−9]

Furthermore, quantum interference effects were explored in excited triplet states both in the absence and in the presence of an external field. For an excited triplet state of low symmetry, the nonstationary character of the initial state was observed through detection of a transient microwave signal following the laser flash.[10] No quantum interference effects were found in the kinetics of growth and decay of photoexcited triplet states in a magnetic field.[11] This may be explained by limited time resolution of the EPR method more than 30 years ago. However, there might be a more fundamental cause. To clarify this problem, we explore the formation of quantum oscillations in an organic triplet state using high-time resolution EPR in combination with pulsed laser excitation.[12]

First, a pulsed EPR experiment is introduced, designed to probe quantum oscillations in the transverse electron spin magnetization. Then, we present angular-dependent X-band EPR studies of triplet pentacene in *p*-terphenyl single crystals. The observed quantum oscillations can be rationalized using an analytical model. Analysis reveals that pulsed light excitation also initiates oscillatory nuclear spin polarization. We report magnetic field-dependent NMR experiments indicating large signal enhancement factors even at very high magnetic fields. This opens new perspectives for the analysis of chemically induced dynamic nuclear polarization (CIDNP) in mechanistic studies of photoactive proteins.

Materials and Methods

Crystal Preparation and Orientation. All chemicals were purchased from Aldrich and were used as received except for protonated *p*-terphenyl, which was further purified by zone refining. Mixed crystals of pentacene in *p*-terphenyl were prepared by the Bridgman technique. The doping ratio was 10^{-3} mol/mol. At room temperature, the *p*-terphenyl crystal is monoclinic with two inequivalent sites in the unit cell. It is assumed that pentacene occupies these sites in a substitutional manner. The crystallographic axes of the host crystal were identified by the conoscopic technique. A sample wedge was used to mount the crystal so that we were able to rotate the pentacene molecule in the **XZ** plane with respect to the static magnetic field, $\mathbf{B}_0$, that is, $0 \leq \theta \leq 180°$, $\phi = 0°$. (See Figure 1.) We checked the crystal orientation by measuring the angular dependence of the echo-induced EPR spectrum of triplet pentacene. Uncertainties in the angles θ and ϕ are estimated to be ± 2 and $\pm 3°$, respectively.

Pulsed EPR Following Pulsed Laser Excitation. To probe the formation of quantum oscillations, we carried out pulsed EPR experiments on an X-band (9.5 GHz/350 mT) EPR spectrometer (Bruker, Elexsys, E680) employing a dielectric resonator with optical access. The crystal was irradiated with pulses of a Nd:YAG laser (Spectra Physics, Quantum-Ray GCR 130-15, 532 nm, 10 mJ/pulse) at a repetition rate of 15 Hz. The laser Q-switch was triggered by the EPR spectrometer, resulting in a maximum jitter of laser flash and microwave pulse of 1 ns.[12] The pulse sequence employed, flash $-t-(2/3)\pi_{mw}-\tau-(2/3)\pi_{mw}-$echo, consists of a short laser pulse (2.5 ns),

[†] Part of the "Michael R. Wasielewski Festschrift".

* To whom correspondence should be addressed. E-mail: gerd.kothe@physchem.uni-freiburg.de.

[‡] University of Freiburg.

[§] Washington University.

[||] Present address: Department of Chemistry, Graduate School of Science and Engineering, Saitama University, 255 Shimo-ohkubo, Sakura-ku, Saitama 338-8570, Japan.

10.1021/jp103508t
Published on Web 07/28/2010

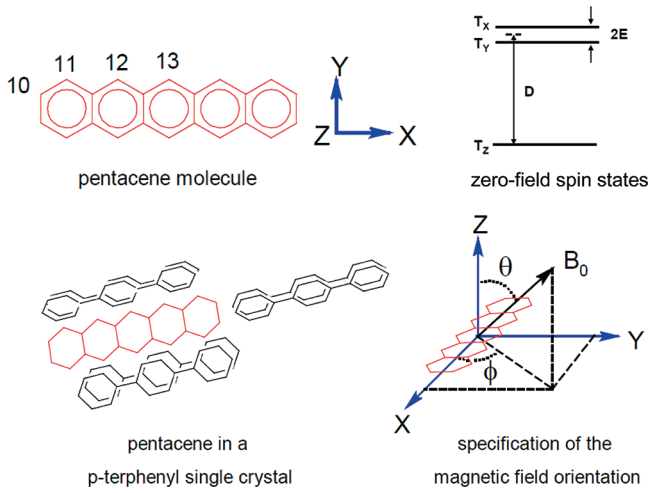

Figure 1. Model system for the study of quantum oscillations in photoexcited triplet states. The studies are performed using single crystals of *p*-terphenyl containing 0.1% of protonated pentacene. Shown is the molecular structure of pentacene together with a coordinate system, **X**,**Y**,**Z**, that diagonalizes the electron dipolar tensor **D**. The numbers 10−13 denote four sets of equivalent protons. We assume that the principal axes of the corresponding hyperfine tensors $\mathbf{A}^{(i)}$ coincide with the molecular symmetry axes. Also shown is a schematic level diagram of the zero-field eigenstates, T_X, T_Y, T_Z, of triplet pentacene, where D and E denote the zero-field splitting parameters. The *p*-terphenyl crystal has two inequivalent sites in the unit cell. which are occupied by pentacene in a substitutional manner. A sample wedge is used to mount the crystal so that one can rotate the pentacene molecule in the **XZ** plane with respect to the static magnetic field $\mathbf{B}_0$, that is, $0 \le \theta \le 180°$, $\phi = 0°$.

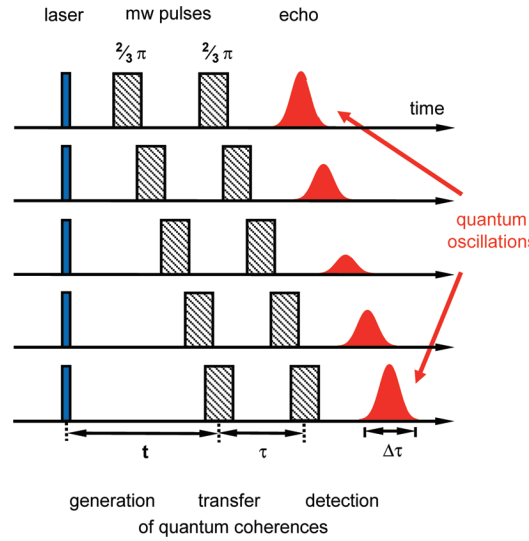

Figure 2. Schematic of a pulsed X-band EPR experiment designed to probe quantum oscillations in photoexcited triplet states. The employed sequence consists of a short laser pulse followed by a variable evolution period, t. At the end of this period, two $(2/3)\pi$ microwave pulses are applied with a fixed pulse separation time, τ. The echo signal at 2τ is then monitored as a function of successively incremented values of t. In this sequence, the laser pulse generates the triplet state and initiates the formation of quantum oscillations, which are then transferred to transverse electron spin magnetization by the two-pulse microwave sequence. Therefore, we expect an oscillatory dependence of the echo signal on the delay, t, between the laser and the first microwave pulse.

followed by a variable evolution period, t. At the end of this period, two $(2/3)\pi$ microwave pulses (16 ns length) are applied with a fixed pulse separation time τ (100 ns). The echo signal at 2τ is then monitored as a function of successively incremented values of t.

Solid-State NMR Combined with Optical Pumping. To detect the light-induced nuclear spin polarization, we performed optical pumping on an X-band EPR spectrometer using a pulsed electron nuclear double resonance (ENDOR) probehead with optical access. The radio frequency circuit of the ENDOR resonator was tuned to a fixed proton frequency of $\omega_N/2\pi$ = 14.52 MHz and connected to a pulsed solid-state NMR spectrometer (Bruker, DSX 300). First, the crystal is irradiated in a variable polarizing field B_0 using a continuous wave laser (532 nm, 500 mW). At the end of the irradiation period (600 s), the magnetic field of the EPR spectrometer is switched adiabatically (∼5 s) to a constant NMR measuring field of B_m = 341.2 mT ($\omega_N/2\pi$ = 14.52 MHz). Finally, the steady-state enhancement factor of the crystal is determined from the amplitude of the free-induction decay (FID), observed under light irradiation and in the dark.

Computations. To analyze the EPR and NMR experiments, numerical calculations were performed using the theoretical model outlined below. The programs calculate the time evolution of the nuclear spin magnetization, $I_x(\Omega,t)$, $I_y(\Omega,t)$, and $I_z(\Omega,t)$, induced in molecular triplet states by pulsed light excitation. Hyperfine interactions with several I = 1/2 nuclei can be considered. In addition, the stationary nuclear spin polarization, $I_z^{stat}(\Omega)$, is calculated after a single excitation cycle on condition of continuous optical pumping. Here we assume a nonselective decay of the triplet state characterized by a single decay constant, $k_X = k_Y = k_Z$. In principle, numerical diagonalization of the spin Hamiltonian allows consideration of nonsecular terms in the calculations. For conceptual reasons, however, the high-field approximation is generally applied.

Results and Discussion

Observation of Quantum Oscillations. The model system for our studies is single crystals of deuterated or protonated *p*-terphenyl containing ∼0.1% of protonated pentacene. Figure 1 depicts the molecular structure of pentacene together with a coordinate system, **X**, **Y**, **Z**, that diagonalizes the electron dipolar tensor **D**. The eigenvalues of **D** can be written as $D_X = -(1/3)\,D + E$, $D_Y = -(1/3)\,D - E$, and $D_Z = (2/3)\,D$, where D and E are the zero-field splitting parameters. The numbers 10−13 denote four sets of equivalent protons in pentacene. For simplicity, we assume that the principal axes of the corresponding hyperfine tensors $\mathbf{A}^{(i)}$ coincide with the molecular symmetry axes. The eigenvalues of $\mathbf{A}^{(i)}$ are denoted by $A_X^{(i)}$, $A_Y^{(i)}$, and $A_Z^{(i)}$. Also shown is a schematic level diagram of the zero-field eigenstates, T_X, T_Y, T_Z, of triplet pentacene. The *p*-terphenyl crystal has two inequivalent sites in the unit cell that are occupied by pentacene in a substitutional manner. A sample wedge was used to mount the crystal, so that we were able to rotate the pentacene molecule in the **XZ** plane with respect to the static magnetic field $\mathbf{B}_0$, that is, $0 \le \theta \le 180°$, $\phi = 0°$.

To probe the formation of quantum oscillations, pulsed X-band EPR experiments were carried out in combination with pulsed laser excitation. A schematic of these experiments is shown in Figure 2. The employed sequence consists of a short laser pulse, followed by a variable evolution period, t. At the end of this period, two $(2/3)\pi$ microwave pulses are applied with a fixed pulse separation time, τ. The echo signal at 2τ is then monitored as a function of successively incremented values of t. In this sequence, the laser pulse generates the triplet state and initiates the formation of quantum oscillations, which are then transferred to transverse electron spin magnetization by

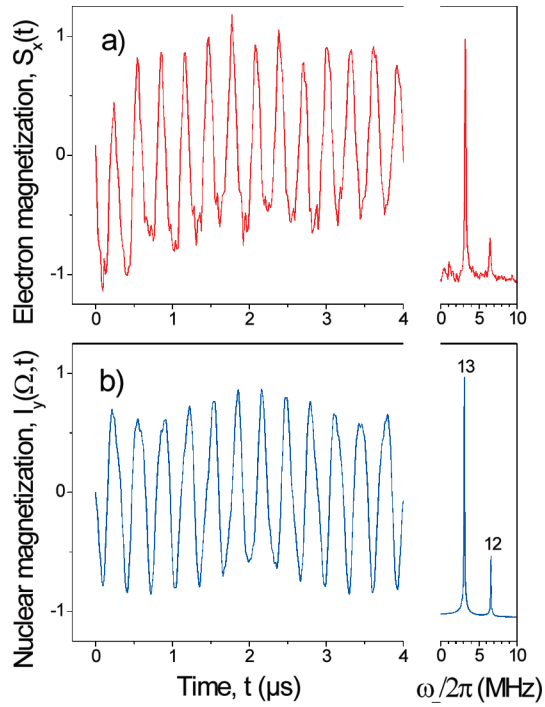

Figure 3. Observing quantum oscillations of nuclear spins in triplet pentacene. To probe the formation of quantum oscillations, pulsed X-band EPR experiments are carried out. The pulse sequence is given in Figure 2. The experiments are performed using protonated pentacene in a deuterated *p*-terphenyl crystal. (a) Experimental quantum oscillations observed in the out-of-phase channel[13] for $\theta = 20°$ at the $T_- - T_0$ EPR transition. The inset shows the magnitude spectrum obtained by Fourier transformation of the time profile. Temperature, $T = 295$ K. (b) Calculated quantum oscillations in the *y*-component of the transverse nuclear magnetization, $I_y(\Omega,t)$ (ω_- NMR transition). Analysis reveals assignment of the quantum coherences to the protons 12 and 13 of triplet pentacene.

the two-pulse microwave sequence. Therefore, we expect that the integrated echo signal has an oscillatory dependence on the delay, t, between the laser and the first microwave pulse.

All EPR experiments were performed at room temperature using protonated pentacene in a deuterated *p*-terphenyl crystal. One observes pronounced oscillations in the EPR time profiles of the in-phase and out-of-phase detection channel.[13] The amplitude and frequency of these oscillations vary with the magnetic field orientation. At canonical orientations, that is, $\mathbf{X} \parallel \mathbf{B}_0$ and $\mathbf{Z} \parallel \mathbf{B}_0$, no oscillations are observed. Figure 3a depicts typical results obtained in the out-of-phase channel.[13] The oscillations refer to $\theta = 20°$ and the $T_- - T_0$ EPR transition. Fourier transformation of the time profile yields the magnitude spectrum shown in the inset on the right. One sees two sharp peaks at 3.2 and 6.5 MHz, which are compatible with ENDOR transitions of proton 13 and 12 in triplet pentacene.[14]

Analytical Theory. The observed oscillations can be rationalized in terms of an analytical model based on the density matrix approach

$$\boldsymbol{\rho}(\Omega,t) = \exp(-i t\mathbf{H}(\Omega)/\hbar)\cdot\boldsymbol{\rho}(\Omega,0)\cdot\exp(i t\mathbf{H}(\Omega)/\hbar) \quad (1)$$

Here $\boldsymbol{\rho}(\Omega,t)$ is the time-dependent density matrix and $\boldsymbol{\rho}(\Omega,0)$ denotes its initial state at the instant of the light pulse. The spin Hamiltonian employed, $\mathbf{H}(\Omega)$, considers Zeeman, dipolar, hyperfine, and nuclear Zeeman interactions of the triplet state. For computational simplicity, hyperfine interactions are restricted to one $I = 1/2$ nucleus. Therefore, $\mathbf{H}(\Omega)$ can be written as

$$\mathbf{H}(\Omega) = g\beta\mathbf{B}_0\cdot\mathbf{S} + \mathbf{S}\cdot\mathbf{D}(\Omega)\cdot\mathbf{S} + \mathbf{S}\cdot\mathbf{A}(\Omega)\cdot\mathbf{I} - g_N\beta_N\mathbf{B}_0\cdot\mathbf{I} \quad (2)$$

where g, β, $\mathbf{S}$, $\mathbf{I}$, g_N, and β_N are the isotropic g factor of the triplet state, the Bohr magneton, the electron spin operator, the nuclear spin operator, the nuclear g factor, and the nuclear magneton, respectively.

Diagonalization of the exponents of eq 1 is achieved using unitary transformations

$$\mathbf{U}^\dagger(\Omega)\cdot(-i\mathbf{H}(\Omega)/\hbar)\cdot\mathbf{U}(\Omega) = \boldsymbol{\Lambda}(\Omega) \quad (3)$$

$$\mathbf{U}^\dagger(\Omega)\cdot(i\mathbf{H}(\Omega)/\hbar)\cdot\mathbf{U}(\Omega) = -\boldsymbol{\Lambda}(\Omega) \quad (4)$$

Substitution of eqs 3 and 4 into eq 1 then gives an explicit expression for the time-dependent density matrix

$$\boldsymbol{\rho}(\Omega,t) = \mathbf{U}(\Omega)\cdot\exp(\boldsymbol{\Lambda}(\Omega)t)\cdot\mathbf{U}^\dagger(\Omega)\cdot\boldsymbol{\rho}(\Omega,0)\cdot\mathbf{U}(\Omega)\cdot \exp(-\boldsymbol{\Lambda}(\Omega)t)\cdot\mathbf{U}^\dagger(\Omega) \quad (5)$$

Finally, we calculate the components of the nuclear spin magnetization in the laboratory frame, $\mathbf{x}$, $\mathbf{y}$, $\mathbf{z}$, with $\mathbf{B}_0$ along the z axis

$$I_j(\Omega,t) = \mathrm{trace}\{\mathbf{I}_j\cdot\boldsymbol{\rho}(\Omega,t)\} \qquad j = x,y,z \quad (6)$$

where $\mathbf{I}_j$ represents the respective nuclear spin operator.

The crucial point is the specification of the initial condition of the triplet state at the instant of the light pulse. It has been generally believed that the nuclear spins are not involved in the ISC process. This implies population of the "pure" zero-field eigenstates of the triplet electrons. However, this approach does not well reproduce the observed quantum oscillations (Appendix A). We then assumed a mixing of the triplet eigenfunctions by the second-order hyperfine interactions in zero-field. With this approach, excellent spectral simulations are obtained. We therefore conclude that the nuclear spins participate in the ISC. Therefore, the initial condition of the triplet state in the molecular frame can be written as

$$\rho(0) = \sum_K p_K|T_K\rangle\langle T_K| \quad (7)$$

where $|T_K\rangle$ are eigenfunctions of the extended zero-field Hamiltonian (Supporting Information)

$$H_{ZF} = \mathbf{S}\cdot\mathbf{D}\cdot\mathbf{S} + \mathbf{S}\cdot\mathbf{A}\cdot\mathbf{I} \quad (8)$$

and p_K denotes the populations of these states immediately after the ISC. In our model, we express the parameters p_K in terms of the population rates p_X, p_Y, and p_Z of the zero-field spin sublevels (Table 1).[15]

Diagonalization of H_{ZF} represented in the high-field triplet basis

TABLE 1: Zero-Field Splitting Parameters and Population Rates of Triplet Pentacene in *p*-Terphenyl Crystals Evaluated by Pulsed EPR[a]

zero-field splitting parameters (MHz)		population rates	
D	1392.2	p_X	0.76
E	−52.92	p_Y	0.16
		p_Z	0.08

[a] Adopted from ref 15.

$$\mathbf{V}^{\dagger}(\Omega)\cdot\mathbf{H}_{ZF}(\Omega)\cdot\mathbf{V}(\Omega) = \mathbf{\Lambda}_{ZF} \tag{9}$$

provides the unitary matrices $\mathbf{V}(\Omega)$ and $\mathbf{V}^{\dagger}(\Omega)$ necessary to transform $\boldsymbol{\rho}(0)$ from the molecular to the laboratory frame (Supporting Information)

$$\boldsymbol{\rho}(\Omega, 0) = \mathbf{V}(\Omega)\cdot\boldsymbol{\rho}(0)\cdot\mathbf{V}^{\dagger}(\Omega) \tag{10}$$

Having specified the initial condition, we can now calculate the response of the triplet state to pulsed light excitation. In the case of an untruncated spin Hamiltonian, theory predicts the formation of quantum oscillations in the electron spin polarization[16] as well as in the transverse and longitudinal nuclear spin magnetization. Using the high-field approximation and perturbation theory in zero-field (Supporting Information), analytical expressions can be derived for the components $I_x(\Omega,t)$, $I_y(\Omega,t)$, and $I_z(\Omega,t)$ of the nuclear magnetization in the laboratory frame. For simplicity, we present the results of a first-order perturbation treatment in which only the leading correction term is retained. Restricting the angular variation of $\mathbf{B}_0$ to the molecular **XZ** plane, $I_x(\Omega,t)$ and $I_y(\Omega,t)$ can be written as

$$I_x(\Omega, t) = -2C\cos^2\theta\left[\frac{B(A+\omega_N)}{\omega_-^2}\sin^2\left(\frac{1}{2}\omega_- t\right) - \frac{B(A-\omega_N)}{\omega_+^2}\sin^2\left(\frac{1}{2}\omega_+ t\right)\right] + C\sin 2\theta\left[\frac{(B^2-\omega_-^2)}{\omega_-^2}\sin^2\left(\frac{1}{2}\omega_- t\right) - \frac{(B^2-\omega_+^2)}{\omega_+^2}\sin^2\left(\frac{1}{2}\omega_+ t\right)\right] \tag{11}$$

$$I_y(\Omega, t) = C\cos^2\theta\left[\frac{B}{\omega_-}\sin(\omega_- t) - \frac{B}{\omega_+}\sin(\omega_+ t)\right] + \frac{1}{2}C\sin 2\theta\left[\frac{(A+\omega_N)}{\omega_-}\sin(\omega_- t) - \frac{(A-\omega_N)}{\omega_+}\sin(\omega_+ t)\right] \tag{12}$$

Here A and B denote the secular part, $A_{zz}(\theta,0°)$, and the pseudosecular part, $A_{zx}(\theta,0°)$, of the hyperfine coupling, ω_+ and ω_- indicate the NMR transitions

$$\omega_{\pm} = [(\omega_N \mp A)^2 + B^2]^{1/2} \tag{13}$$

of the given nucleus in the T_+ and T_- state, and $\omega_N = g_N\beta_N B_0/\hbar$ is the nuclear Larmor frequency.

TABLE 2: Proton Hyperfine Tensor Elements of Triplet Pentacene in *p*-Terphenyl Crystals Evaluated by Pulsed ENDOR[a]

	principal values of the hyperfine tensor (MHz)		
proton position i	$A_X^{(i)}$	$A_Y^{(i)}$	$A_Z^{(i)}$
10	−3.75	−0.75	−2.64
11	−2.80	−1.00	−3.04
12	−12.65	−3.94	−9.86
13	−19.84	−6.53	−14.34

[a] Adopted from ref 14.

From eqs 11 and 12, one can see that the modulation amplitude of the nuclear quantum oscillations consists of two parts that have a different physical origin. The first part, $C = (1/8)A_Z(p_Y - p_X)/E$, results from the mixing of the electron spin functions by the second-order hyperfine interactions in the zero field.[2,17] The second part, including $B(A+\omega_N)/\omega_-^2$, $B(A-\omega_N)/\omega_+^2$, $(B^2-\omega_-^2)/\omega_-^2$, and $(B^2-\omega_+^2)/\omega_+^2$, is due to the mixing of the nuclear spin functions by the pseudosecular hyperfine coupling in the presence of a magnetic field. Because of the latter process, the modulation amplitude sensitively depends on the chosen B_0. Maximum amplitude is expected if the nuclear Zeeman frequency matches the secular hyperfine coupling

$$|\omega_N| = |A| \tag{14}$$

Furthermore, the model predicts a vanishing amplitude for canonical orientations of the hyperfine tensor because at these orientations the pseudosecular hyperfine term vanishes, that is, $B(0°,0°) = B(90°,0°) = 0$.

In general, the formation of the nuclear quantum oscillations can be rationalized as follows: The ISC selectively populates the eigenstates of the extended zero-field Hamiltonian including a hyperfine term. Thus, initially, the nuclear spins are aligned along a molecular axis. Then, the spins suddenly experience the external magnetic field. This leads to a nonadiabatic change of the spin quantization axis, $[\rho(0),H] \neq 0$, and to the formation of nuclear quantum oscillations.[18]

Identification of Nuclear Spin Oscillations. To identify the observed oscillations, numerical calculations were performed using the theoretical model outlined above. The molecular symmetry of pentacene suggests consideration of two equivalent protons in the spin Hamiltonian.[1] Yet, basically the same results were obtained for a single proton. In principle, numerical diagonalization of the spin Hamiltonian allows consideration of nonsecular terms in the calculations. For conceptual reasons, however, the high-field approximation is generally applied. Within this approximation, numerical and analytical calculations yield very similar results.

Analysis suggests that the experimental oscillations, observed in the out-of-phase channel[13] (Figure 3a), can be assigned to the y component of the transverse nuclear magnetization, $I_y(\Omega,t)$. For a given field and orientation ($B_0 = 383.8$ mT, $\theta = 20°$), the frequency and amplitude of the nuclear spin oscillations are determined by the hyperfine parameters of the various nuclei. For pentacene, these parameters are known from a recent ENDOR study.[14] (See Table 2.) Using these values, we obtain the modulation curve and magnitude spectrum shown in Figure 3b. The oscillations refer to the ω_- NMR transition. Exceptionally, nonsecular terms were also considered in the calculation. The agreement with the experiment is excellent. Therefore, for the first time, nuclear quantum oscillations have been observed in an excited triplet state.

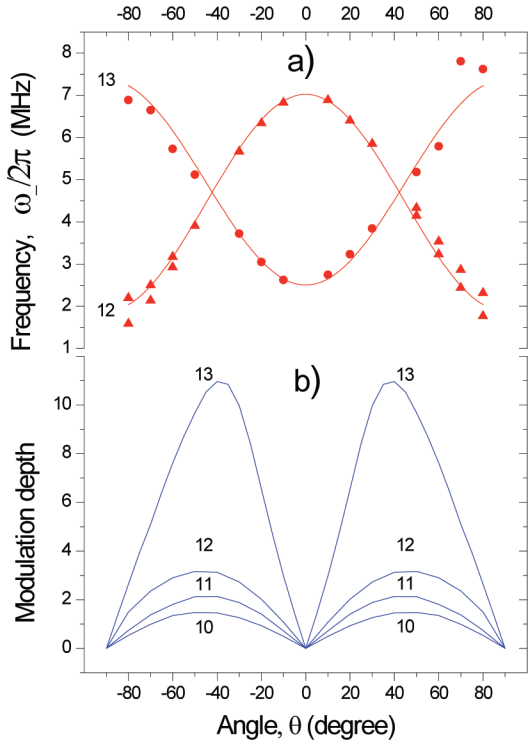

Figure 4. Quantum oscillations of protonated triplet pentacene in a deuterated *p*-terphenyl crystal. (a) Experimental oscillation frequencies of the protons 12 (▲) and 13 (●) as a function of the rotation angle θ. The quantum oscillations are observed in the out-of-phase channel[13] of a pulsed EPR experiment at the $T_- - T_0$ transition. Temperature, T = 295 K. (b) Calculated modulation amplitudes of the protons 10−13 as a function of the rotation angle θ. The calculation refers to the *y*-component of the transverse nuclear magnetization $I_y(\Omega,t)$ (ω_- NMR transition) and predicts a vanishing amplitude for canonical orientations of the hyperfine tensor, that is, for θ = 0 and 90°.

The study reveals assignment of the quantum coherences to the protons 12 and 13 of triplet pentacene. Figure 4a shows the oscillation frequencies of these protons measured as a function of the rotation angle θ at the $T_- - T_0$ EPR transition. The solid lines are eye fits to the experimental data points. In Figure 4b, we depict the modulation amplitudes of the protons 10−13, calculated as a function of the rotation angle θ. Again, only the results for the ω_- NMR transition are shown. Two characteristic features can be noted. First, the model predicts a vanishing amplitude for canonical orientations of the hyperfine tensor. Clearly, this is in agreement with the experimental findings. Second, the model predicts a progressive decrease in the modulation amplitude starting from proton 13. Basically, only oscillations from the protons 13 and 12 are observed. They exhibit the largest hyperfine couplings that approximately satisfy the matching condition

$$B_0 = B_{\text{match}} = |A\hbar|/|g_N\beta_N| \qquad (15)$$

in X-band EPR experiments. The protons 11 and 10 have considerably smaller hyperfine couplings and thus can hardly be detected anymore.

Oscillatory Nuclear Spin Polarization. The mechanism responsible for the formation of light-induced transverse nuclear magnetization also acts as a source of oscillatory longitudinal nuclear magnetization

$$I_z(\Omega,t) = 2C\cos^2\theta\left[\left(\frac{B}{\omega_-}\right)^2\sin^2\left(\frac{1}{2}\omega_- t\right) - \left(\frac{B}{\omega_+}\right)^2\sin^2\left(\frac{1}{2}\omega_+ t\right)\right] + C\sin 2\theta\left[\frac{B(A+\omega_N)}{\omega_-^2}\sin^2\left(\frac{1}{2}\omega_- t\right) - \frac{B(A-\omega_N)}{\omega_+^2}\sin^2\left(\frac{1}{2}\omega_+ t\right)\right] \qquad (16)$$

Figure 5a depicts a model calculation for $I_z(\Omega,t)$ of proton 13 in triplet pentacene. The calculation refers to a rotation angle of θ = 20° and a magnetic field of B_0 = 350 mT. For convenience, $I_z(\Omega,t)$ is normalized to the thermal polarization I_z^{eq} at 350 mT and room temperature. Notably, $I_z(\Omega,t)$ oscillates about a large average value of −15 000 times the thermal polarization, indicating a huge NMR signal enhancement factor of $\varepsilon = I_z^{av}(\Omega)/I_z^{eq} = -15\,000$. Fourier transformation of $I_z(\Omega,t)$ yields the magnitude spectrum shown in the inset on the right. One sees two peaks at 2.0 and 29.9 MHz, which indicate the two NMR transitions, ω_- and ω_+, of proton 13.

Figure 5b shows the magnetic field dependence of the enhancement factor $\varepsilon = I_z^{av}(\Omega)/I_z^{eq}$ calculated for the protons 10, 12, and 13 of triplet pentacene in the field range of B_0 = 0 to 1 T. The calculation refers to a rotation angle of θ = 20°. For simplicity, $I_z^{av}(\Omega)$ is normalized to a constant thermal polarization of $I_z^{eq} = 1.0 \times 10^{-6}$, corresponding to a magnetic field of 350 mT and room temperature. One sees that the enhancement factor of each proton exhibits a distinct emissive maximum at lower magnetic fields.

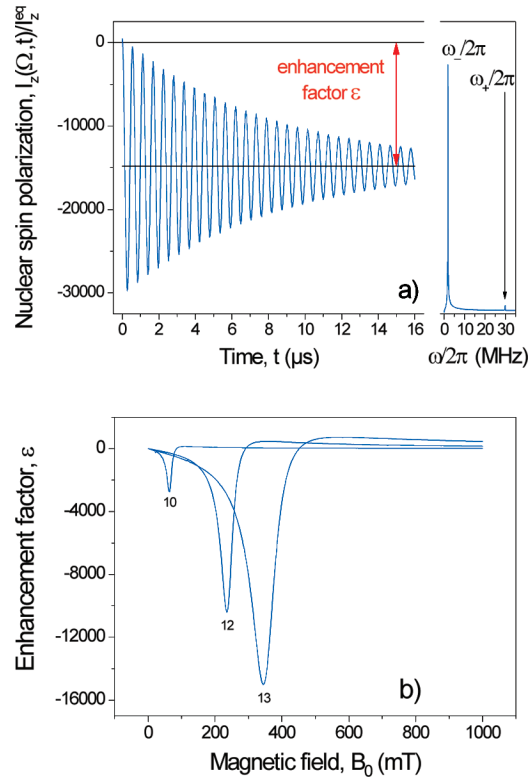

Figure 5. Prediction of oscillatory nuclear spin polarization in photoexcited triplet states. (a) Model calculation for $I_z(\Omega,t)$ of proton 13 in triplet pentacene. The calculation refers to a magnetic field of B_0 = 350 mT and θ = 20°. $I_z(\Omega,t)$ is normalized to the thermal polarization I_z^{eq} at B_0 = 350 mT and room temperature. The two sharp peaks in the magnitude spectrum indicate quantum oscillations of proton 13 at B_0 = 350 mT and θ = 20°. (b) Calculated NMR signal enhancement factor, $\varepsilon = I_z^{av}(\Omega)/I_z^{eq}$, for the protons 10, 12, and 13 of triplet pentacene in the field range of B_0 = 0 to B_0 = 1 T. The calculation refers to a rotation angle of θ = 20°. Maximum emissive polarization is expected if the nuclear Larmor frequency matches the secular hyperfine coupling, $|\omega_N|$ = |A|.

To rationalize the calculation, we consider only the first and third terms of eq 16, which provide the major contribution to $I_z^{av}(\Omega)$. The first term yields an emissive polarization independent of B_0, $\mathrm{sgn}(C) = \mathrm{sgn}(A_Z)\ \mathrm{sgn}(E)\ \mathrm{sgn}(p_Y - p_X) = -1$, whereas the third term gives an emissive/absorptive polarization pattern with a change of sign at B_{match}. Therefore, for $B_0 \leq B_{match}$ we expect a negative nuclear polarization independent of the magnetic field orientation θ. A maximum of $I_z^{av}(\Omega)$ is predicted at the matching field $B_{match} = |A\hbar|/|g_N\beta_N|$. Proton 10 has the smallest hyperfine parameters and thus shows the lowest matching field. In contrast, proton 13 has the largest hyperfine parameters and consequently exhibits the highest matching field. For $B_0 > B_{match}$, the third term of eq 16 becomes dominant. Therefore, if $B_0 \gg B_{match}$, then we expect a linear dependence of $I_z^{av}(\Omega)$ on the inverse strength of the magnetic field, $I_z^{av}(\Omega) \sim B_0^{-1}$. This weak field dependence guarantees large enhancement factors even at very high magnetic fields.

NMR Signal Enhancement. To detect the light-induced nuclear spin polarization, pulsed NMR experiments were performed in combination with optical pumping. First, the crystal is irradiated in a variable polarization field B_0 using a continuous wave laser. The irradiation generates nuclear spin polarization in the pentacene molecules. After the decay of the triplet state, the polarization is transferred to the *p*-terphenyl molecules via spin diffusion. At the end of the irradiation period (600 s), determined by the proton spin−lattice relaxation time of the crystal ($T_1 = 120$ s), the magnetic field of the EPR spectrometer is switched adiabatically to a constant NMR measuring field of $B_m = 341.2$ mT. Finally, the steady-state enhancement factor of the crystal, $\varepsilon_{cryst} = (I_{light} - I_{dark})/I_{dark}$, is determined from the amplitude of the FID, observed under light irradiation and in the dark. The effective crystal enhancement factor at the polarizing field B_0, $\varepsilon_{cryst}^{eff}$, can be determined from ε_{cryst} according to $\varepsilon_{cryst}^{eff} = \varepsilon_{cryst}B_m/B_0$ (high-temperature approximation).

All NMR experiments were performed at room temperature using protonated pentacene in a protonated *p*-terphenyl crystal. Figure 6a depicts the enhancement factor of the crystal, ε_{cryst}, measured as a function of the rotation angle θ. The experiments refer to a polarizing field of $B_0 = 900$ mT. For comparison, we calculated the stationary enhancement factor of pentacene, $\varepsilon_{pent} = I_z^{stat}(\Omega)/I_z^{eq}$, after a single excitation cycle (Appendix B). The calculation considers all 14 protons of pentacene as well as the two inequivalent sites of the crystal. The result is displayed in Figure 6b. The calculated curve reproduces the observed orientation dependence remarkably well.

Figure 7a shows the enhancement factor of the crystal, measured as a function of the polarization field in the range of $B_0 = 0$ to 1 T. The experiments refer to a rotation angle of $\theta = 120°$. As predicted by the model calculations (Figure 5b), ε_{cryst} exhibits several emissive maxima at lower magnetic fields, then goes through zero, builds up a broad absorptive maximum, and finally decreases again. In Figure 7b, we show the magnetic field dependence of ε_{pent}, calculated on the basis of our model (Appendix B). The numbers 10−13 indicate the matching field of the various protons. One sees that the calculated curve is in reasonable agreement with the observed magnetic field dependence. This suggests that the underlying theoretical model is basically correct.

From Figure 7a, we extract a crystal enhancement factor of 3.6 at 1 T. Because of the doping ratio of 0.1% and an NMR measuring field of 0.341 T, this corresponds to an effective enhancement factor of 1100 for pentacene. Evidently, high nuclear spin polarization is created in triplet states solely by light excitation. The formation of this polarization is a consequence of the ISC process and does not require intense microwave irradiation. We note that optical nuclear polarization (ONP) in triplet states was observed over 30 years ago.[19,20] However, the mechanism proposed for the formation of ONP is somewhat different. Present analysis suggests a mixing of the "pure" triplet eigenstates by the second-order hyperfine interactions in the zero field. As a result, large NMR signal enhancement factors are induced, even at very high magnetic fields.

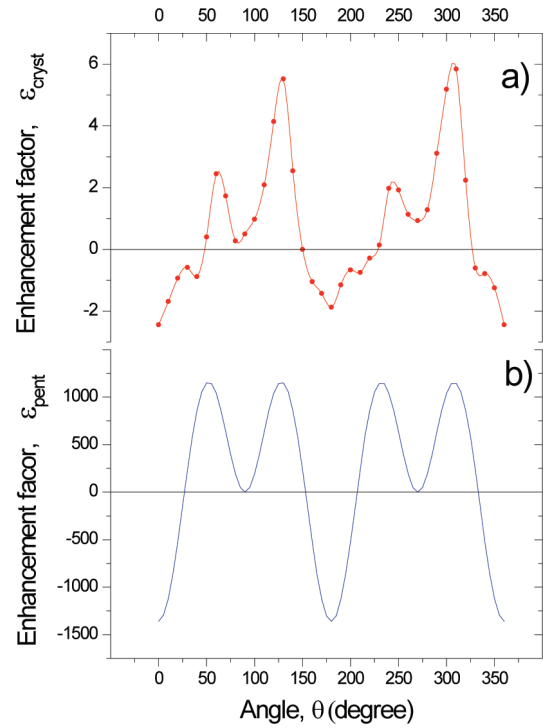

Figure 6. Detection of light-induced nuclear spin polarization from triplet pentacene. The experiments are performed using protonated pentacene in a protonated *p*-terphenyl crystal. First, the crystal is irradiated for a given time in a variable polarizing field B_0 using a continuous wave laser. At the end of the irradiation period, B_0 is switched adiabatically to a constant NMR measuring field B_m. Finally, the steady-state enhancement factor of the crystal, $\varepsilon_{cryst} = (I_{light} - I_{dark})/I_{dark}$, is determined from the amplitude of the FID, observed under light irradiation and in the dark. (a) Experimental enhancement factor of the crystal, ε_{cryst}, measured as a function of the rotation angle θ. The experiments refer to a polarizing field of $B_0 = 900$ mT and $T = 295$ K. (b) Calculated stationary enhancement factor of pentacene, $\varepsilon_{pent} = I_z^{stat}(\Omega)/I_z^{eq}$, after a single excitation cycle.

Let us now assume that the cofactor of a photoactive protein has similar triplet properties as pentacene and calculate the steady-state enhancement factor in a high-field CIDNP experiment under the condition of continuous optical pumping (Appendix B). Considering a magnetic field of 7 T and evaluating the powder average, we obtain an effective enhancement factor of $\varepsilon_{cofact}^{eff} \approx -4$. Similar values have been observed for the blue-light receptor phototropin reconstituted with a ^{13}C-labeled cofactor.[21] This shows that triplet states can be a major source for CIDNP in mechanistic studies of photoactive proteins.

In general, photochemistry in these proteins proceeds via spin-correlated radical pairs formed either in a singlet or in a triplet state.[22,23] The resulting spin configuration depends on the photophysical properties of the excited cofactor. If, initially, a singlet radical pair is formed, then the observed photo-CIDNP can be analyzed using a radical pair mechanism.[22−25] For a triplet

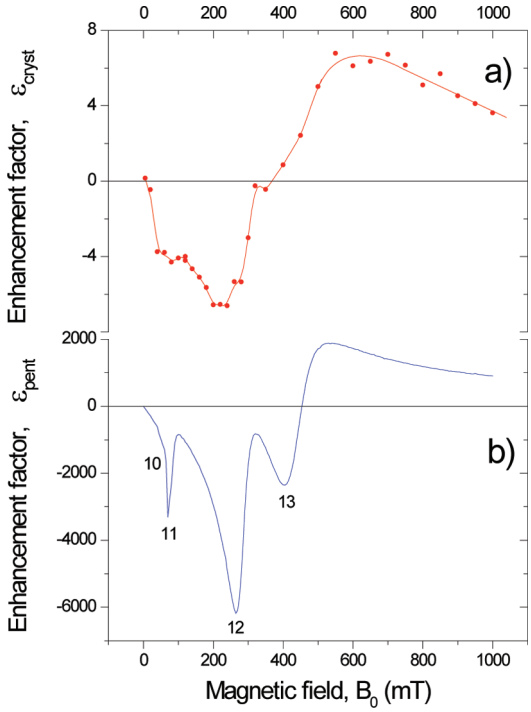

Figure 7. Light-induced nuclear spin polarization from protonated triplet pentacene in a protonated *p*-terphenyl crystal on condition of continuous optical pumping. (a) Experimental steady-state enhancement factor of the crystal, $\varepsilon_{cryst} = (I_{light} - I_{dark})/I_{dark}$, as a function of the polarizing field B_0. The experiments refer to a rotation angle of $\theta = 120°$ and $T = 295$ K. (b) Calculated stationary enhancement factor of pentacene, $\varepsilon_{pent} = I_z^{stat}(\Omega)/I_z^{eq}$, after a single excitation cycle. The numbers 10−13 indicate the matching condition of the various protons.

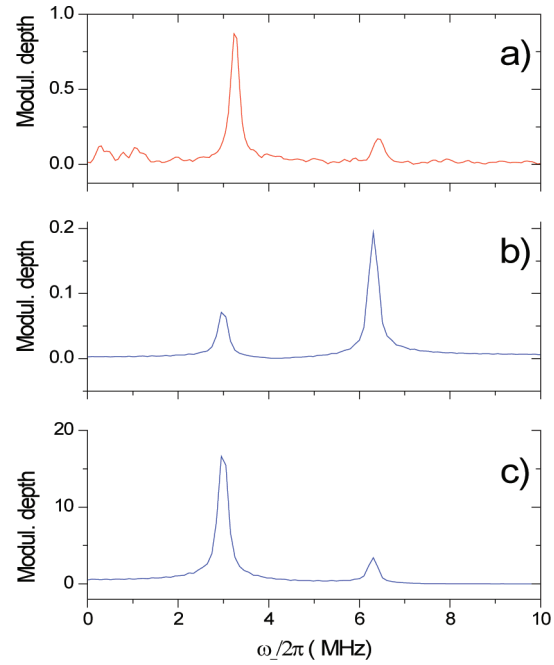

Figure 8. Quantum oscillations of protonated triplet pentacene in the transverse nuclear spin magnetization $I_y(\Omega,t)$. (a) Experimental magnitude spectrum observed in the out-of-phase channel[13] of a pulsed EPR experiment for $\theta = 20°$ at the $T_- - T_0$ transition. (b) Calculated magnitude spectrum assuming the "conventional" ISC mechanism. (c) Calculated magnitude spectrum assuming that the nuclear spins are actively involved in the ISC process.

radical pair, however, the spin dynamics in the precursor state should also be considered. This requires a more comprehensive analysis involving both a radical pair and a triplet mechanism. We believe that this approach is necessary for a number of photoactive proteins, to unravel the electron transfer pathways and to identify the redox partners involved in the protein function.

Conclusions

We have observed quantum oscillations of nuclear spins in photoexcited triplet states using pulsed EPR in combination with pulsed laser excitation. The quantum coherences can be rationalized on the basis of an analytical theory. Analysis reveals that immediately after the ISC, the nuclear spins are aligned along a molecular axis. Then, the spins suddenly experience the external magnetic field. This leads to a nonadiabatic change of the spin quantization axis and to the formation of nuclear quantum oscillations.

The novel mechanism also acts as a source of oscillatory nuclear spin polarization that gives rise to large NMR signal enhancement factors, even at very high magnetic fields. This opens new perspectives for the analysis of CIDNP in mechanistic studies of photoactive proteins. If, initially, a singlet radical pair is formed, then the observed photo-CIDNP can be analyzed using a radical pair mechanism.[22−25] In the case of a triplet radical pair, however, the spin dynamics in the precursor state should also be considered. This requires a more comprehensive analysis involving the new triplet mechanism of the present study.

Acknowledgment. We would like to thank T. Berthold for excellent technical assistance. G. K. acknowledges financial support from the Ministry of Science, Research and the Arts of Baden-Württemberg.

Appendix A: Initial Condition of the Triplet State

It has been generally believed that the nuclear spins are not involved in the ISC process. This implies population of the "pure" zero-field eigenstates of the triplet electrons. In the Figure 8a,b, we compare experimental quantum oscillations of triplet pentacene with those calculated using the "conventional" mechanism. Clearly, this approach does not well reproduce the experimental observations. In Figure 8c, we assume that hyperfine interactions of the nuclear spins contribute to the ISC. With this approach, an excellent spectral simulation is obtained.

Appendix B: Stationary Nuclear Spin Polarization

In this Appendix, we evaluate the stationary nuclear spin polarization, $I_z^{stat}(\Omega)$, of triplet molecules after a single excitation cycle using a numerical solution of the stochastic Liouville equation[26,27]

$$\frac{\partial}{\partial t}\boldsymbol{\rho}(\Omega,t) = -i\{(1/\hbar)[\mathbf{H}(\Omega),\boldsymbol{\rho}(\Omega,t)] - i\mathbf{K}(\Omega)\cdot\boldsymbol{\rho}(\Omega,t)\} \quad \text{(B-1)}$$

Here $\boldsymbol{\rho}(\Omega,t)$ is the time-dependent spin density matrix,

$$\mathbf{H}(\Omega) = g\beta\mathbf{B}_0\cdot\mathbf{S} + \mathbf{S}\cdot\mathbf{D}(\Omega)\cdot\mathbf{S} + \mathbf{S}\cdot\mathbf{A}(\Omega)\cdot\mathbf{I} - g_N\beta_N\mathbf{B}_0\cdot\mathbf{I} \quad \text{(B-2)}$$

is the relevant spin Hamiltonian, and $\mathbf{K}(\Omega)$ denotes a kinetic operator, which describes the decay of the triplet state. Assuming that the triplet sublevels decay nonselectively

$$k_X = k_Y = k_Z = k \tag{B-3}$$

the kinetic operator is given by

$$\mathbf{K}(\Omega) = k\mathbf{E} \tag{B-4}$$

and eq B-1 can be integrated to

$$\boldsymbol{\rho}(\Omega, t) = \exp(-kt)\exp(-it\mathbf{H}(\Omega)/\hbar)\cdot\boldsymbol{\rho}(\Omega, 0)\cdot \exp(it\mathbf{H}(\Omega)/\hbar) \tag{B-5}$$

where $\boldsymbol{\rho}(\Omega,0)$ is the initial condition of the triplet state at the instant of the light pulse. (See eqs 7−10.)

The exponents of eq B-5 can be diagonalized using unitary transformations. Substitution of eqs 3 and 4 into eq B-5 gives an explicit expression for the time-dependent density matrix

$$\boldsymbol{\rho}(\Omega, t) = \exp(-kt)\mathbf{U}(\Omega)\cdot\exp(\boldsymbol{\Lambda}(\Omega)t)\cdot\mathbf{U}^{\dagger}(\Omega)\cdot \boldsymbol{\rho}(\Omega, 0)\cdot\mathbf{U}(\Omega)\cdot\exp(-\boldsymbol{\Lambda}(\Omega)t)\cdot\mathbf{U}^{\dagger}(\Omega) \tag{B-6}$$

which is readily evaluated using a complex diagonalization routine. Finally, we calculate the stationary nuclear spin polarization after a single excitation cycle according to

$$I_z^{\mathrm{stat}}(\Omega) = k\int_0^{t_{\max}} \mathrm{trace}\{\mathbf{I}_z\cdot\boldsymbol{\rho}(\Omega, t)\}\,\mathrm{d}t \tag{B-7}$$

With the assumed decay dynamics, no significant triplet population is left after $5/k$; therefore, it is sufficient to compute the time evolution of $\boldsymbol{\rho}(\Omega,t)$ up to $t_{\max} = 5/k$. For transient triplet states, embedded in host crystals, $I_z^{\mathrm{stat}}(\Omega)$ is a good approximation to the steady-state polarization that builds up on condition of continuous optical pumping.[20] We believe that this is also true for triplet intermediates in photoactive proteins.

Supporting Information Available: A short presentation of the perturbation treatment used to evaluate the eigenvalues and eigenvectors of the triplet spin Hamiltonian in zero-field. A brief description of the analytical method used to transform the initial density matrix from the molecular to the laboratory frame. A short account of the high-field approximation employed to diagonalize the triplet spin Hamiltonian in the presence of a magnetic field. This material is available free of charge via the Internet at http://pubs.acs.org.

References and Notes

(1) Van der Waals, J. H.; de Groot, M. S. Magnetic Interactions Related to Phosphorescence. In *The Triplet State*; Zahlan, A. B., Ed.; Cambridge University Press: Cambridge, U.K., 1967; pp 101−132.
(2) Köhler, J.; Disselhorst, J. A. J. M.; Donckers, M. C. J. M.; Groenen, E. J. J.; Schmidt, J.; Moerner, W. E. *Nature* **1993**, *363*, 242–244.
(3) Wrachtrup, J.; von Borczyskowski, C.; Bernard, J.; Orrit, M.; Brown, R. *Nature* **1993**, *363*, 244–245.
(4) Henstra, A.; Lin, T.-S.; Schmidt, J.; Wenckebach, W. T. *Chem. Phys. Lett.* **1990**, *165*, 6–10.
(5) Schmidt, J.; van den Heuvel, D. J.; Henstra, A.; Lin, T.-S.; Wenckebach, W. T. *Isr. J. Chem.* **1992**, *32*, 165–172.
(6) Iinuma, M.; Takahashi, Y.; Shaké, I.; Oda, M.; Masaike, A.; Yabuzaki, T. *Phys. Rev. Lett.* **2000**, *84*, 171–174.
(7) Kouskov, V.; Sloop, D. J.; Weissman, S. I.; Lin, T.-S. *Chem. Phys. Lett.* **1995**, *232*, 165–168.
(8) Yang, T.-C.; Sloop, D. J.; Weissman, S. I.; Lin, T.-S. *J. Chem. Phys.* **2000**, *113*, 11194–11201.
(9) Yang, T.-C.; Sloop, D. J.; Weissman, S. I.; Lin, T.-S. *Chem. Phys. Lett.* **2000**, *331*, 489–496.
(10) Nonhof, C. J.; Plantenga, F. L.; Schmidt, J.; Varma, C. A. G. O.; van der Waals, J. H. *Chem. Phys. Lett.* **1979**, *60*, 353–357.
(11) Felix, C. C.; Weissman, S. I. *Proc. Natl. Acad. Sci. U.S.A.* **1975**, *72*, 4203–4204.
(12) Kothe, G.; Bechtold, M.; Link, G.; Ohmes, E.; Weidner, J.-U. *Chem. Phys. Lett.* **1998**, *283*, 51–60.
(13) In rotating frame experiments, out-of-phase detection implies to record the EPR signal in phase with the rotating microwave field. In general, the amplitude of the quantum oscillations in the out-of-phase channel is by a factor of two larger than that in the in-phase channel.
(14) Yago, T.; Link, G.; Kothe, G.; Lin, T.-S. *J. Chem. Phys.* **2007**, *127*, 114503.
(15) Sloop, D. J.; Yu, H.-L.; Lin, T.-S.; Weissman, S. I. *J. Chem. Phys.* **1981**, *75*, 3746–3757.
(16) Yago, T.; Weidner, J.-U.; Link, G.; Lin, T.-S.; Kothe, G. *Chem. Phys. Lett.* **2007**, *438*, 351–357.
(17) Brouwer, A. C. J.; Köhler, J.; Groenen, E. J. J.; Schmidt, J. *J. Chem. Phys.* **1996**, *105*, 2212–2222.
(18) Salikhov, K. M. *Chem. Phys. Lett.* **1993**, *201*, 261–264.
(19) Colpa, J. P.; Hausser, K. H.; Stehlik, D. *Z. Naturforsch.* **1971**, *26a*, 1792–1799.
(20) Stehlik, D. The Mechanism of Optical Nuclear Polarization in Molecular Crystals. In *Excited States*; Lim, E. C., Ed.; Academic Press: New York, 1977; Vol. 3; pp 203−303.
(21) Richter, G.; Weber, S.; Römisch, W.; Bacher, A.; Fischer, M.; Eisenreich, W. *J. Am. Chem. Soc.* **2005**, *127*, 17245–17252.
(22) Kaptein, R.; Dijkstra, K.; Nicolay, K. *Nature* **1978**, *274*, 293–294.
(23) Hore, P. J.; Broadhurst, R. W. *Prog. Nucl. Magn. Reson. Spectrosc.* **1993**, *25*, 345–402.
(24) Polenova, T.; McDermott, A. E. *J. Phys. Chem. B* **1999**, *103*, 535–548.
(25) Jeschke, G.; Matysik, J. *Chem. Phys.* **2003**, *294*, 239–255.
(26) Kubo, R. A Stochastic Theory of Line Shape. In *Stochastic Processes in Chemical Physics*; Schuler, K.; Ed.; Advances in Chemical Physics 15; Wiley: New York, 1969; pp 101−127.
(27) Freed, J. H.; Bruno, G. V.; Polnaszek, C. F. *J. Chem. Phys.* **1971**, *75*, 3385–3399.

JP103508T